AFRC 2023 Industrial Combustion Symposium
Denver, Colorado
September 25–27, 2023

Swiss-roll Combustor: An Innovative Enclosed Combustor for high Methane Destruction Efficiency and Ultra-low NO_X Emissions

Authors: Daksh Adhikari[1], Patharapong Bhuripanyo[2], Parthib Rao[1], Patryk Radyjowski[1], Chien-Hua Chen[1] and Paul Ronney[2]

[1]Advanced Cooling Technologies, Inc., Lancaster, PA, USA

[2]University of Southern California, Los Angeles, CA, USA

1. Introduction

Methane is a powerful greenhouse gas with a global warming potential (over 100 years) at least 25 times that of CO_2. Regulators in the U.S. and the world aim to reverse the rate of accumulation of methane in the atmosphere and thus ameliorate the harmful effects of climate change. According to the EPA Green House Gas Inventory, oil and gas production, gathering and processing account for a large share of the total methane emissions (second only to enteric fermentation). Open (assisted and non-assisted) and enclosed flares are typically used to mitigate methane and other VOC emissions.

While large capacity flares that are associated with process emergency/safety have been under scrutiny, smaller capacity non-emergency flares have received less attention. According to the Texas Railroad Commission, in 2017, there were roughly 97,000 flares in Texas. Out of these, about a third burn less than 20 MCF/day, about half of the flares burn less than 50 MCF/day, and less than 10% burn more than 400 MCF/day.[1] Existing small-capacity open flares (<100 MCF/day) suffer from low (<95%) methane destruction efficiency and are more susceptible to variability in performance due to wind and varied gas composition. Moreover, small enclosed combustors must overcome significant challenges to meet current and future NOx emission limits. Achieving high methane destruction efficiency and low NOx emissions across a broad operational range, particularly in applications like flaring that involve highly variable conditions including high turndown ratios and gas composition fluctuations, poses practical and economical challenges. Emissions of unreacted methane from insufficient maintenance and suboptimal operation of current combustion control devices have been reported as one of the leading factors in emissions. Addressing these challenges often necessitates including complicated and expensive control systems, thereby escalating both capital and operational costs with the aforementioned technologies. Therefore, there remains a distinct need for a simple, robust combustion system that can achieve near 100% destruction efficiency over a wide range of gas stream composition and flow rates while minimizing NOx and other emissions (e.g., soot, PM 2.5). The Swiss roll combustor (SRC) is one such technology that can potentially address these challenges.

2. Swiss roll Combustor Technology

The so-called 'Swiss-roll' combustor is a unique device that incorporates heat recuperation by wrapping the combustion zone with a spiral counterflow heat exchanger between the inlet (unburned reactants) and outlet (burned product) streams. It was first proposed by Dr. Felix Weinberg in 1974; since then, many studies have demonstrated its unique performance capabilities.[2-7] As shown in **Figure 1A**, an air stream enters the center combustion chamber through a long spiral inlet channel, and the gas stream enters the central combustion chamber near the center where sufficient mixing can be achieved. This is a slight variation on the devices employed by Weinberg and most others, where the fuel and air are mixed outside the device and only a single inlet flow path of premixed reactants exists. In the device shown in **Figure 1A**, combustion air can be provided using either a blower or a natural draft. After the combustion process, the hot products flow out through an adjacent outlet channel. The heat of combustion from the hot products of combustion is transferred to the incoming air across the wall of the heat exchanger. The combustion products are then exhausted at a temperature well below that of the reaction zone due to the transfer of heat from the product to the reactant stream. By exchange of enthalpy between hot products and cooler reactants, the combustion temperature can attain values above that corresponding to the adiabatic flame temperature associated with reactants at ambient temperature (that is, super-adiabatic temperatures), which increases the reaction rate which in turn leads to wider flammability limits and more complete reaction for a given mixture. **Figure 1B** and **Figure 1C** illustrate how super-adiabatic temperatures can be achieved in the center of the spiral heat exchanger. Without heat recirculation, the reaction temperature increase is from the chemical reaction only, but with heat recirculation, the reaction temperature is increased due to both the chemical reaction and heat transfer. This elevated reaction temperature can enable a stable, nearly complete reaction even with low heating value reactant streams. In other words, the excess enthalpy reaction extends the flammability limits of the fuel and enables ultra-lean, self-sustained combustion, eliminating the supplemental fuel that would otherwise be needed to incinerate low-BTU waste gas streams.

Due to the large reaction zone area in the center of the Swiss roll compared to a propagating flame, the combustion inside the Swiss-roll can be sustained at a temperature lower than typical combustion, which in turn reduces NOx formation significantly. Previous experiments using a sub-scale Swiss-roll (1 ft x 1 ft) showed between 0-1 ppm NOx emission.[8]

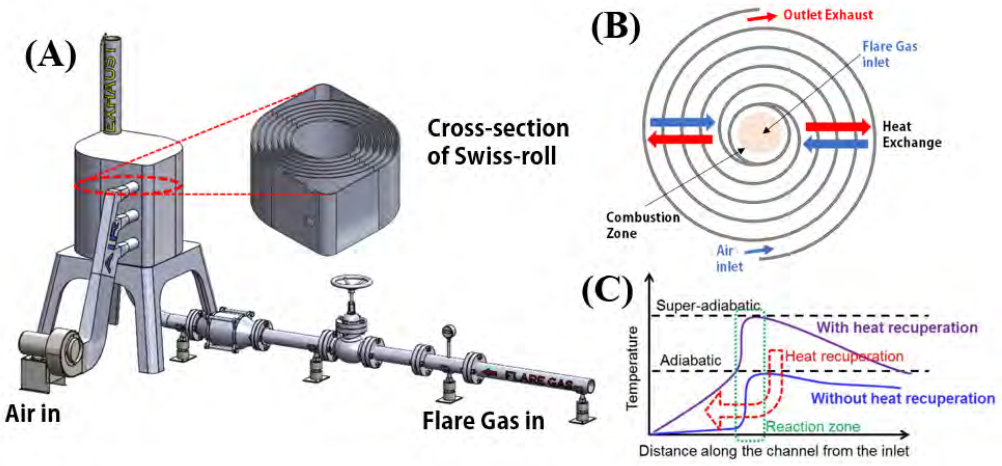

Figure 1. ***(A)*** *Schematic of Swiss roll Enclosed Combustor for flare gas incineration;* ***(B)*** *Overview of Swiss roll concept.* ***(C)*** *Temperature profiles of the combustor with and without heat recirculation.*

3. Objectives

The challenges and potential solutions related to the use of Swiss roll combustors (SRC) in flare gas incineration are examined using Computational Fluid Dynamics (CFD) models in a variety of operating conditions. We focus on key factors including the pressure drop, the impact of heat recirculation on extinction limits across different scales, transient behavior during operation, and the quantification of destruction efficiency alongside NOx formation. Non-reacting flow simulations are used to gain insight into the relationships between system geometry, heat recirculation, and pressure drop, aiding in system optimization. Reacting flow simulations are used to examine combustion performance and extinction limits at different scales. Furthermore, the system's performance under severe transient conditions, like sinusoidal oscillations and single-pulse fluctuations in flowrate, is assessed.

This work presents an overview of the operational principles and unique features of the SRC, alongside the numerical modeling conducted to understand the factors influencing pressure drop and the effects of heat recuperation on combustion efficiency and emissions. Our main objective is to highlight the potential of Swiss roll combustors in flare gas incineration and contribute to the future advancement of more efficient, cleaner combustion systems.

4. CFD Modeling Setup

Two broad types of computational fluid dynamics-based studies were undertaken to aid the design of the Swiss roll. First was a series of steady-state, 2D and 3D simulations *without reaction chemistry* that aimed at finding the optimal design space (e.g. number of turns) in the Swiss roll between the effectiveness of heat recirculation and the pressure drop for practical applications. The feasibility of a natural-draft based Swiss roll is also investigated. Second, was a series of 2D transient simulations *with detailed reaction chemistry* aimed at investigating the Swiss roll's transient characteristics and flame stability under surge and oscillatory waste gas flows.

4.1 Simulation Setup for Steady-State Flow Model without Reaction

A steady-state, thermo-fluidic CFD model was used to rapidly iterate designs and explore geometric scale-up effects. Air with temperature-dependent properties was used as the working fluid. The thermal effects of combustion were represented by a cylindrical zone with a fixed temperature in the core, as a first-order estimate for the typical temperature expected during operation, while avoiding the need to fully resolve the combustion in the CFD model. The model included radiation and a custom expression for the out-of-plane heat loss.[5] Reynolds Stress models (RSM) were employed in solving the turbulent flow field. The outer wall was set at a 10 W/m^{2}K heat transfer coefficient to ambient temperature (300K) and the wall's external emissivity. A velocity or a pressure inlet condition was used, along with a pressure outlet (**Figure 3A**). The pressure inlet condition is used for a fully passive Swiss roll design, where the required air flow rate is provided by the natural draft due to the buoyant effects in the exhaust stack/chimney (**Figure 3B**).

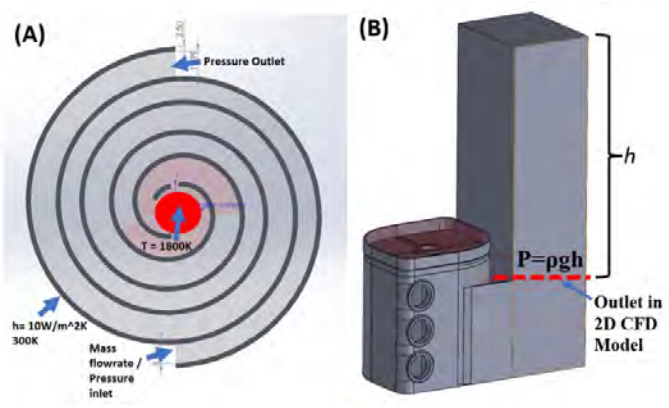

Figure 3. (A) *Setup for steady state CFD model.* ***(B)*** *3D Representation of pressure outlet.*

4.2 Simulation Setup for Transient Detailed Chemistry Combustion Model

A set of time-dependent simulations were carried out to (i) examine the Swiss roll combustor's capabilities to withstand upstream flare fluctuations, and (ii) determine key transient considerations which will influence the design space of the Swiss roll combustors.

For the reaction-enabled CFD simulations, the setup is 2D, transient, and includes the effects of temperature-dependent gas and solid properties. The viscous effects are modeled using the Reynolds Stress Model (RSM). Surface-to-surface radiation was modeled via the discrete ordinates method. The detailed GRI-Mech III (53 Species, 325 reactions)[9] is used as the primary gas-phase combustion model in the CFD model, although other global reaction mechanisms are also used as appropriate to reduce the computational cost. The outermost surface heat loss to ambient (300K) is modeled via natural convection with a 10 W/m^{2}K heat transfer coefficient and 0.8 wall external emissivity. The out-of-plane volumetric heat sink's thermal resistance model[5] (**Figure 4B**) assumes a 1cm ceramic insulation block and 0.5 mm aluminum support structure to mimic typical experimental configuration. The inlet boundary is a fixed mass-flow inlet with ambient temperature reactants (premixed combustion). Reasonable measures were taken to ensure grid/timestep independent results, and conservation of mass, species, and energy was verified.

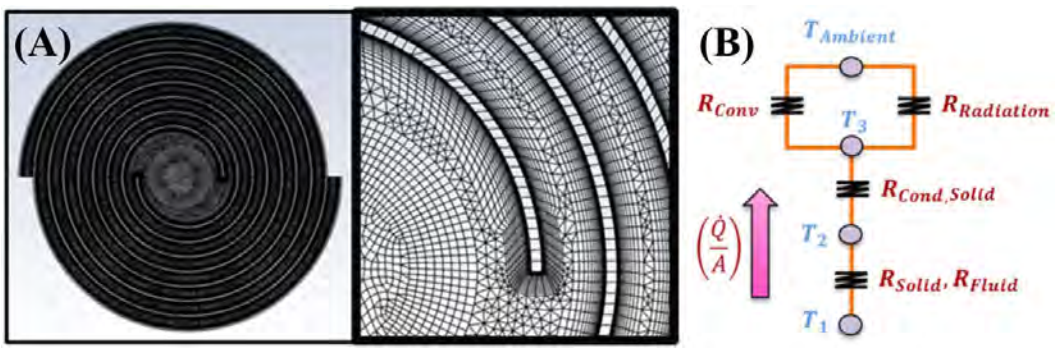

Figure 4. (A) *Representative mesh for 2D CFD model.* ***(B)*** *Visualization of out-of-plane heat loss model.*

5. Results & Discussion

5.1 Scaling Factor for Mass Flow and Overall Pressure Drop

The goal of this initial study was to establish the relationship between mass flow rate and pressure drop between sub-scale and larger geometries. Three different sizes of Swiss roll were examined: 6”x6” (laboratory-scale), 10”x10” (sub-scale), and 24”x24” (full-scale). The 6”x6” and 10”x10” geometry, shown in **Figure 5,** were compared at multiple flow rates with steady state 2D CFD simulations.

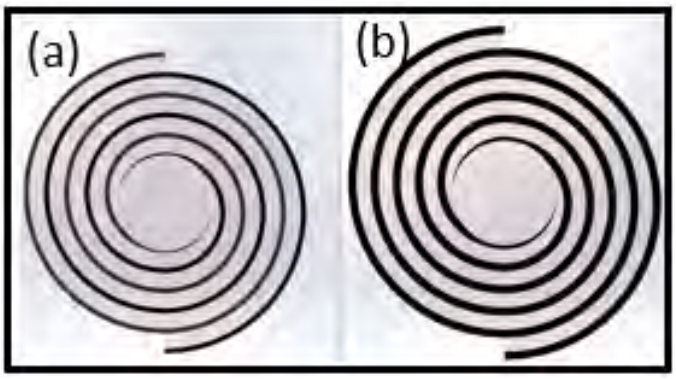

Figure 5: (A) *6” and* ***(B)*** *10” Swiss roll. (Not to scale)*

The ratio of hydraulic diameter (D_h) squared was used as the scaling factor between the different geometries (*Equation 1*). The flow rates used for the inlet boundary conditions for the sub-scale models were based on the full-scale flow rates expected for a 24”x24” geometry and scaled down based on Equation 1. The 24” Swiss roll had a target waste/flare gas capacity of 100 MSCFD and the sub-scale models were scaled down proportionately. **Table 1** shows the scaled mass flow rates used in the CFD model.

$$[1] \quad \dot{m}_2 = \dot{m}_1 \left(\frac{D_{h,2}}{D_{h,1}}\right)^2$$

Table 1. *Scaled Total Mass Flow Rates*

Full Scale (24") Flowrate [MSCFD]	400	550	700	850	1000
Lab Scale (6") Flowrate [MSCFD]	35	47	59	71	82
Sub Scale (10)" Flowrate [MSCFD]	84	111	139	167	195

The overall pressure drop (air inlet – outlet) corresponding to scaled flow rates is shown in **Figure 6**. The Δp between the 6”x6” and 10”x10” models are very similar, indicating that the flow rate has been scaled correctly. Note the geometry used in this study was not optimized for reducing pressure drop.

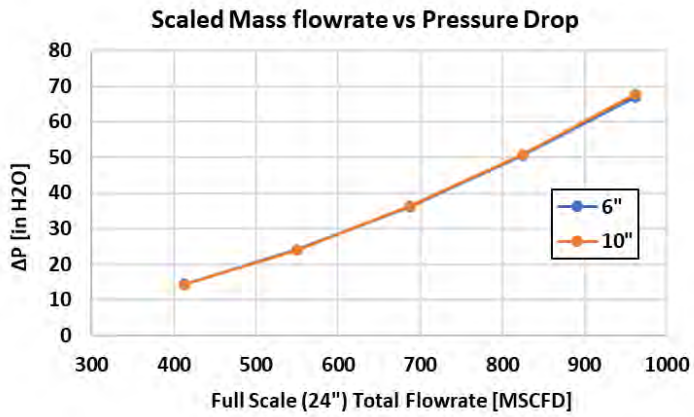

Figure 6: *The 6" and the 10" models have the same ΔP with the correctly scaled total mass flow.*

Thus, it can be concluded that the correct scaling factor between smaller sub-scale models and larger geometries is indeed the ratio of hydraulic diameter squared. These results indicate that the hydraulic diameter squared based scaling factor can be used to model the hydrodynamic effects inside the Swiss roll, and thus smaller computational domains can be used for CFD models for estimating hydrodynamic performance for the full-scale.

5.2 Natural Draft Driven (Passive) Swiss-roll

As an alternative to the forced-air system, the Swiss roll configuration can be optimized to be used as a completely passive system. Natural-draft (passive) systems are often preferable over forced-draft systems in cases where there is a *steady* stream of waste gases, especially of low heating value. They are cheaper to install and operate- features that are important for flaring in remote locations. Since it is common practice to employ an exhaust chimney for ground-mounted enclosed combustors, the effect of buoyancy is leveraged in the design phase. If the pressure drop in the inner channels can be overcome by the buoyancy effect that arises from the chimney at the outlet, a negative pressure difference from the inlet to the outlet will provide the driving force for airflow.

To investigate the effect of buoyancy, two different steady-state CFD models of a 24" Swiss roll were used. Design A (**Figure 7A**) is designed to be used with an active blower to provide the required airflow for combustion, whereas Design B (**Figure 7B**) is designed to be a fully passive system that uses the airflow generated by the natural draft effect, eliminating the need for any forced airflow. Design A had more turns and narrower channel widths compared to Design B. Thus, Design A will have more heat recirculation than Design B, however, it will also have a larger pressure drop. For the fully passive system (B), the low-pressure drop design allows the system to use the effect of buoyancy from the stack effect at the outlet to provide the necessary airflow.

The boundary condition for Design A was a prescribed inlet mass-flow rate, and a pressure outlet corresponding to an exhaust height of 20 feet (calculated using $P=\rho gh$). For Design B the inlet was set at atmospheric pressure, and the outlet was a pressure outlet corresponding to different exhaust heights.

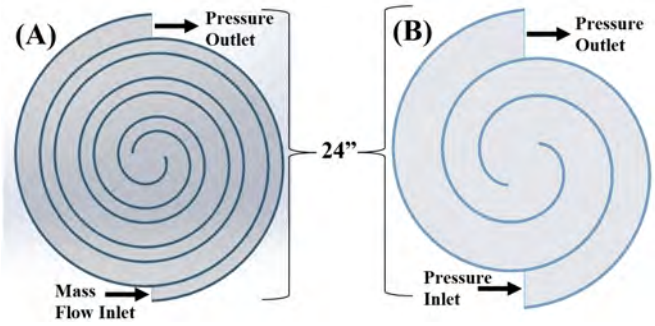

Figure 7. (A) *Design A: 24" Swiss roll designed for use with forced airflow.* ***(B)*** *Design B: Fully Passive Swiss roll (No forced airflow required). Note the fewer turns in (B) compared to (A)*

Design A uses different inlet and outlet channel widths (1 inch and 1.8 inches, respectively) to reduce the pressure drop from the center core, where the flare gas enters, to the outlet- to accommodate the supply pressure of flare gas stream. Since this design operates with forced airflow from a blower, it can afford larger pressure drops compared to Design B. The mass-flow rate at the inlet was varied and the corresponding air and fuel (flare gas) pressure drops for Design A are shown in **Figure 8A**. The air pressure drop is taken as the Δp from the inlet to the outlet and the fuel (flare gas) pressure drop is from the center core to the outlet. The total flow rate and pressure drops at different stack heights for Design B are shown in **Figure 8B**. For the fully passive system (Design B), the total flow rate will increase with a taller exhaust height due to a larger pressure difference from the buoyancy effect. The passive system further reduces the internal pressure drop by increasing the channel widths and reducing the number of turns in the combustor.

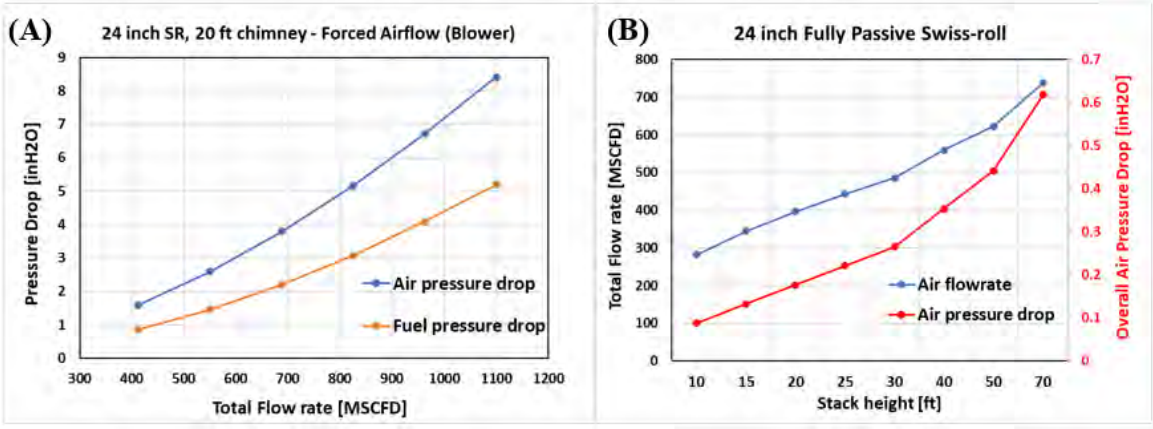

Figure 8: (A) *Air (from inlet) and fuel (from center) pressure drop vs total flow rate (air+fuel) for forced airflow model (Design A in Figure 7).* ***(B)*** *Total flow rate vs stack height and overall pressure drop for fully passive Swiss roll model (Design B in Figure 7).*

The pressure drops for the passive system are much lower than the forced airflow system at the same flow rates. For example, at a stack height of 20 feet and total flow rate of 400 MSCFD, Design A (with blower) has a total air pressure drop of almost 10x of Design B (fully passive), ~1.5 inH_2O vs ~0.175 inH_2O, which is attributed to the narrower channel walls in Design A.

Although wider channels in Design B are beneficial from a pressure drop standpoint, they negatively impact the heat recirculation ability of the Swiss roll due to less heat transfer area. This can be seen in the temperature contours for the forced airflow (**Figure 9A**) and passive system (**Figure 9B**). Larger inlet and outlet channels and fewer turns in Design B cause a reduction in the heat recirculation capability of the passive Swiss roll. At the same flow rate, Design A can preheat the inlet fluid from 300K to ~800K, while Design B does not raise the temperature significantly. This decrease in heat recirculation may increase the lower bounds of the lean extinction limit that is achievable with the passive Swiss roll, however, this type of system may prove to be ideal for applications with steady flare/waste gas flow rates and composition, especially if the equivalence ratio is expected to remain near the stoichiometric value. In such cases, the DRE is generally high, so the heat recirculation isn't as important and the reduction in costs with a fully passive system (no blower required) are expected to outweigh the costs of preheating the incoming fluid.

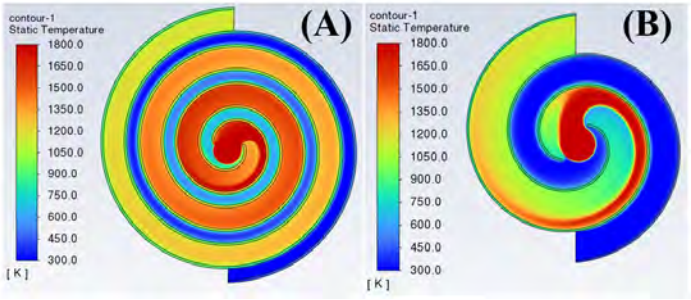

***Figure 9**: Temperature contour for the **(A)** forced airflow and **(B)** passive Swiss roll at 400 MSCFD total flow rate. The heat recirculation increases with the number of turns.*

The models show that the flowrate and pressure drop can be controlled by the exhaust stack height, channel widths and number of turns, which in turn affect the heat recirculation capability. In applications with low waste gas flow rate, where the DRE is generally low due to the low combustion temperatures, more turns can be added to preheat the reactants and thus increase combustion efficiency.

5.3 Performance of Sub-Scale (10" x 10") Swiss-roll.

Swiss roll's capability to burn at extreme conditions outside traditional mixture (methane-air) flammability limits ($\Phi = 0.4, 3.0$) was demonstrated through a series of transient simulations with detailed methane-air chemistry (GRI-Mech III). The geometry includes two different designs under the same fabrication constraints (minimum feature size, estimated core size, material, etc.), one with 2.5 turns and 3.5 turns (**Table 2**). The operations were simulated at high total flow rate cases (30,000 SCFD [Re=2,577] - 117,000 SCFD [Re=10,309] total (air + flare gas flow rates) to demonstrate recirculation capabilities required under targeted conditions.

***Table 2** Geometrical dimensions for different models*

Dimensions	2.5 turns	3.5 turns
Overall Size [cm]	25.4	25.4
Simulated Height [cm]	22.0	22.0
Est. Core Diameter [cm]	7.2	6.0
Channel Width [cm]	1.3	1.0
Wall Thickness [cm]	0.2	0.2

The contour plots of fluid temperature, solid temperature, and heat of reaction for 2.5 turns at Φ = 0.4, 3.0 are provided in **Figure 10** and **Figure 11** respectively.

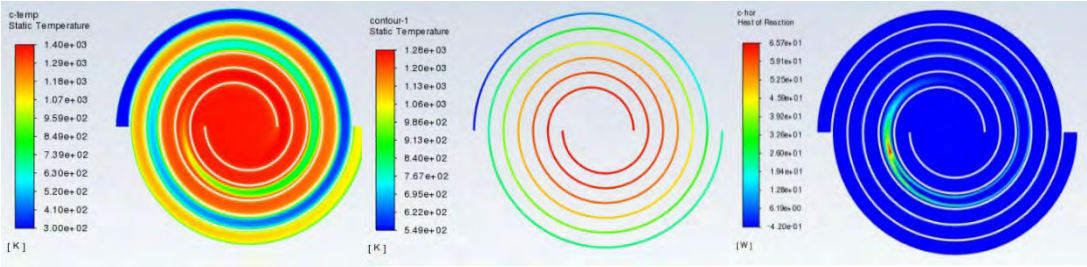

Figure 10. (Left) *Fluid temperature,* ***(Center)*** *solid temperature, and* ***(Right)*** *heat of reaction for 2.5 turns, 10-inch Swiss roll operating at Φ = 0.4, Re = 2577*

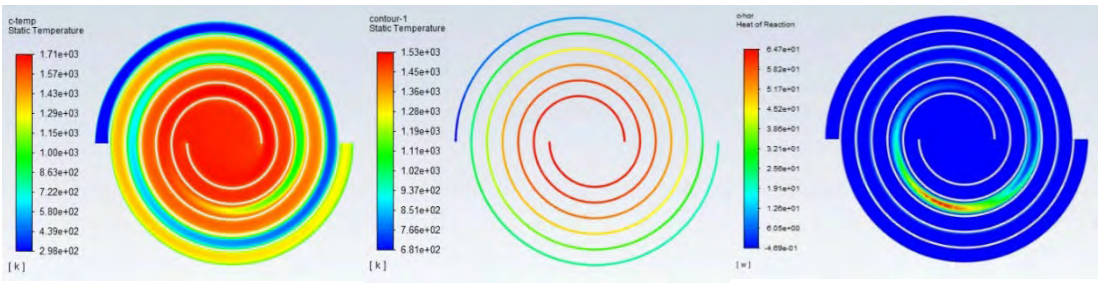

Figure 11*. (Left)* *Fluid temperature,* ***(Center)*** *solid temperature, and* ***(Right)*** *heat of reaction for 2.5 turns, 10-inch Swiss roll operating at Φ = 3.0, Re = 2577*

Both figures show solutions converged at out-of-center regions, suggesting that the 2.5 turn geometry can support even leaner/richer mixtures at this flow rate. However, at 117,000 SCFD [Re = 10,309], the flame could not sustain itself at Φ = 0.4, at which the centered flame propagated further down the outlet channel and eventually became extinguished over a 7-second duration.

The 3.5 turns results, shown in **Figure 12**, provide a sustaining flame converged solution at 4 times higher flow rate compared to 2.5 turns at the same mixture composition Φ = 0.4. The increase in excess enthalpy capacity comes at the cost of increased pressure drop. This highlights how effectively managing the pressure drop budget in the design will be key to meeting the pressure drop requirements.

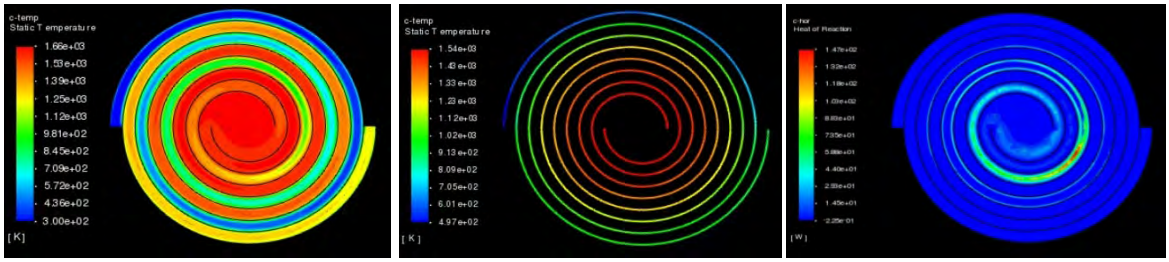

Figure 12. (Left) *Fluid temperature,* ***(Middle)*** *solid temperature, and* ***(Right)*** *heat of reaction for 3.5 turns, 10-inch Swiss roll operating at Φ=0.4, Re = 10,309*

5.4 Oscillatory Flow Response

Swiss roll's capability to support mild continuous steady-oscillations of overall flow rate was examined through a series of transient simulations with detailed methane-air chemistry (GRI-Mech III). The specific geometry involved 3.5 turns, and a 3" Swiss roll combustor (5cm height, 3mm channel width, 0.5mm wall thickness, and 22mm core diameter). Steady sinusoidal oscillatory profiles of varying magnitudes (Amplitude Factor (A) $\equiv$ $maximum\ flowrate\ amplitude/\ mean\ flowrate$) and frequencies (f) were imposed to inlet flow rate at varying compositions to determine the change in effective extinction limits due to such disturbances.

The lean extinction limit ($\emptyset_{ext}$) , quantifies the minimum amount of fuel required to sustain combustion, and serves as a primary indicator of the heat-recirculation performance of Swiss roll combustors. The limit is generally dependent on the scale and operating flow rate (*Re*); however, the dependency is significantly less pronounced at high flow rates as residence time dictates the extinction behavior in such regimes. Consequently, the study is focused on a single value for mean flow rate of 30,000 SCFD (Re = 2577).

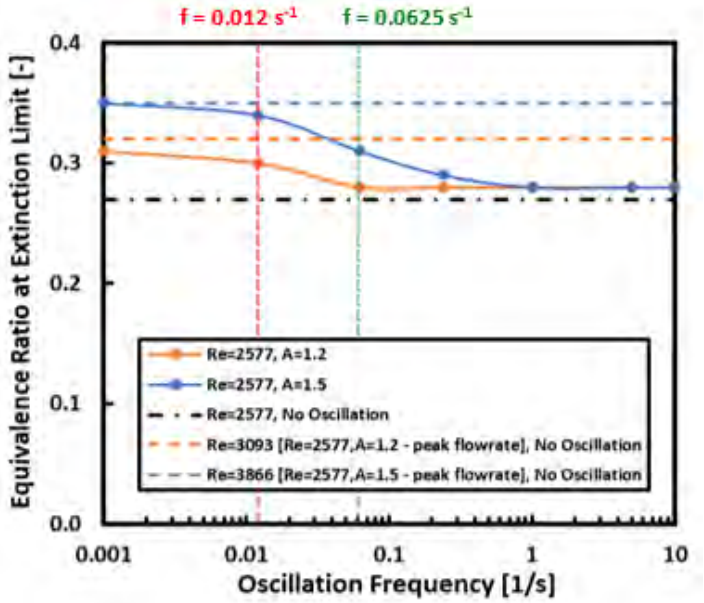

Figure 13: *Effective extinction limits for high flow rate case under steady mass flow oscillations of varying amplitude factors and frequencies for ¼-ft scale Swiss roll combustor with detailed methane chemistry.*

The results are shown in **Figure 13**, where oscillating extinction limits were found to be practically identical to steady-state extinction limits at sufficiently high frequencies across the cases explored. However, towards lower oscillation frequencies, the extinction limits become narrower as heat loss timescales can catch up. An estimated typical quasi-steady flare profile (f = 0.0625 s^{-1}, A = 1.5 [turndown ratio = 3]), would require ~14.6% additional fuel mass compared to steady operations. For very slow oscillations, the performance plateaus, and the oscillating extinction limits resemble the quasi-steady limits corresponding to flow rate peaks for high Re cases. The inverse is true for low flow rate (low Re) cases (not shown) but instead, the extinction would plateau to the minimum flow rate troughs for low oscillation frequencies.

5.5 Flare Surge Study

Separate transient studies were conducted with increasing flare gas mass flow under constant air mass flow rate (hence overall flow rate changes), representing more abrupt, intense changes that are typical for flares. The goal is to simulate flare surges and observe the SRC's response in extreme

cases without considering air-flow rate adjustments or intervention via a control system. The methane mass flow surges are modeled via Gaussian-type functions $f(t) = f_0 + (f_{max} - f_0) \exp\left[-\frac{(t-(b+t_0))^2}{2c^2}\right]$ (applied separately to overall mass flow, and inlet species compositions). The geometry and models used here are the same as the prior oscillatory study. Different surge profiles (different amplitudes, periods) were investigated. The transient profiles were applied to steady-state converged results near the lean extinction limit (Re = 1546, Φ = 0.22) where the flame is centered. Example of surge inlet profiles for Φ_{peak} = 2.0, T_{Surge} = 8s are provided in **Figure 14**.

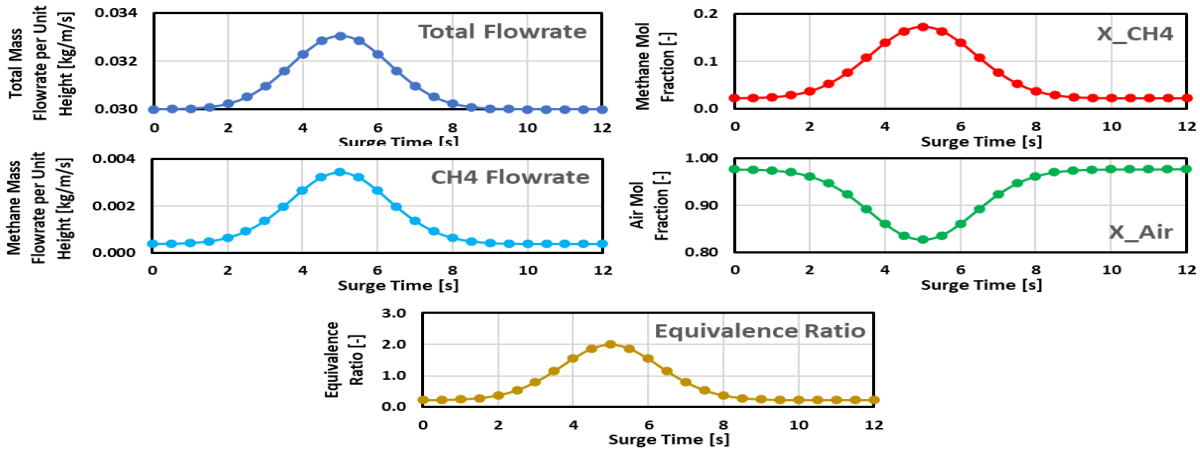

Figure 14: Simulated surge profile (flow rates, composition) for Φ_{peak} = 2.0, T_{Surge} = 8s applied after simulated-steady initial conditions $Re_{initial}$ = 1546, $\Phi_{initial}$ = 0.22.

Figure 15 shows the global maximum temperatures in each fluid and solid zone and the comparison with instantaneous steady-state results (correspond to calculations where the mixtures at such points are kept constant and running until time-independent results are obtained). $\emptyset_{peak}$ = 1.0 and $\emptyset_{peak}$ = 3.0 translates to peak methane amplitudes of approximately 5-fold and 14-fold increase from the initial limit condition. The temperature profile for the rich mixture displays two separate temperature spikes as the device passes through stoichiometry on two separate occasions. Note that the flame and its location respond extremely fast to upstream changes, which the solid phase noticeably lags behind as to be expected from convection delay. There are significant gaps between transient and steady-state maximum wall temperatures, which can serve as a buffer (thermal mass) provided a short surge duration. Thus, the CFD models show a delay in the thermal response of the solid, which can allow the potential control system to respond in sufficient time and control the temperature by increasing the air flow rate.

The species profiles for T_{Surge} = 8s are shown in **Figure 16** for $\emptyset_{peak}$ = 1 and $\emptyset_{peak}$ = 3, which are practically symmetrical. The values closely follow instantaneous steady-state solutions even at such rapid surge timescales as there are practically no time delays for flames' responses. For lean and near-stoichiometric mixtures, DRE performances are promising. For very rich mixtures, the results show a slight amount of excess methane, as well as reformed hydrogen as a product of fuel-rich pathways.

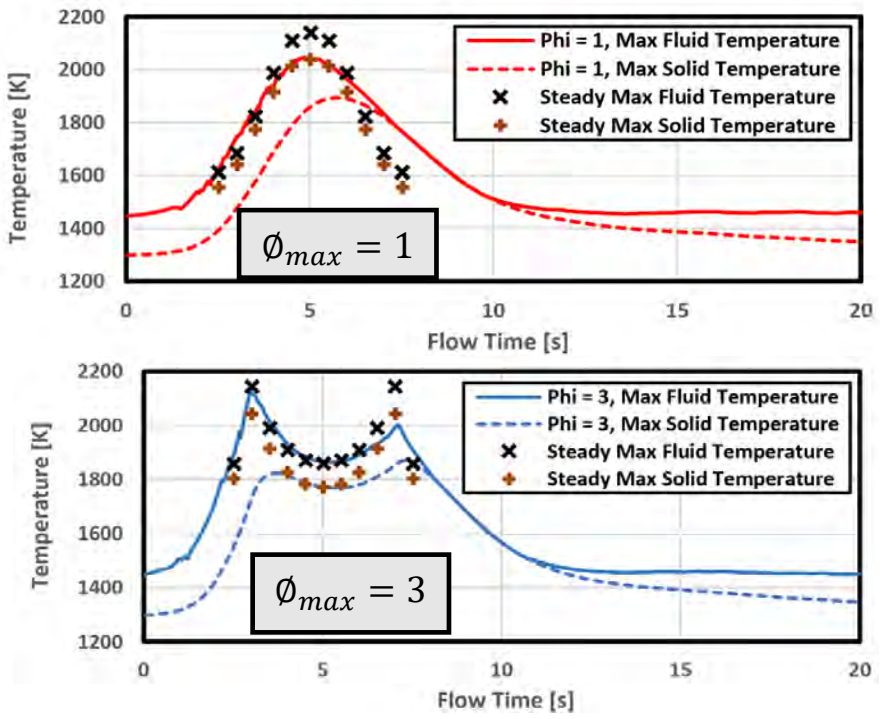

Figure 15: Simulated transient and steady-state comparisons between maximum gas and solid temperature responses of ¼-ft scale Swiss roll combustor operating at lean-limit to 8-seconds methane surges with (Top) $\emptyset_{peak}$ = 1 and (Bottom) $\emptyset_{peak}$ = 3 under constant air mass flow at *Re* = 1546.

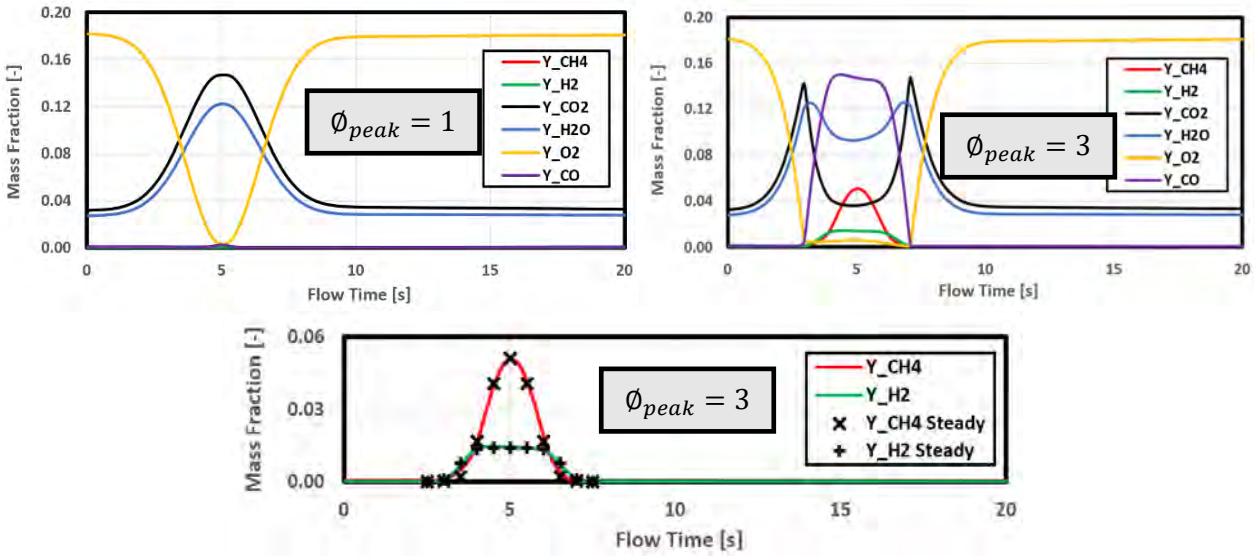

Figure 16: Species response profile with T_{Surge} = 8s for (**Top-Left**) $\emptyset_{peak}$ = 1.0 and (Top-Right) $\emptyset_{peak}$ = 3.0, with (**Bottom**) comparison to steady-state conditions.

The wall's temperature profiles at four different locations for $\emptyset_{peak}$ = 2.0 and T_{Surge} = 32s are provided in **Figure 17**. Note that despite the flame readily retreating far upstream into inlet channels during the surge, the temperature still increases at centered locations due to increasing mixture strength. For less rapid surge timescales, the wall's temperature profile is expected to shift such that the highest wall temperature would coincide with the flame's location, and the center part of the walls are expected to cool down.

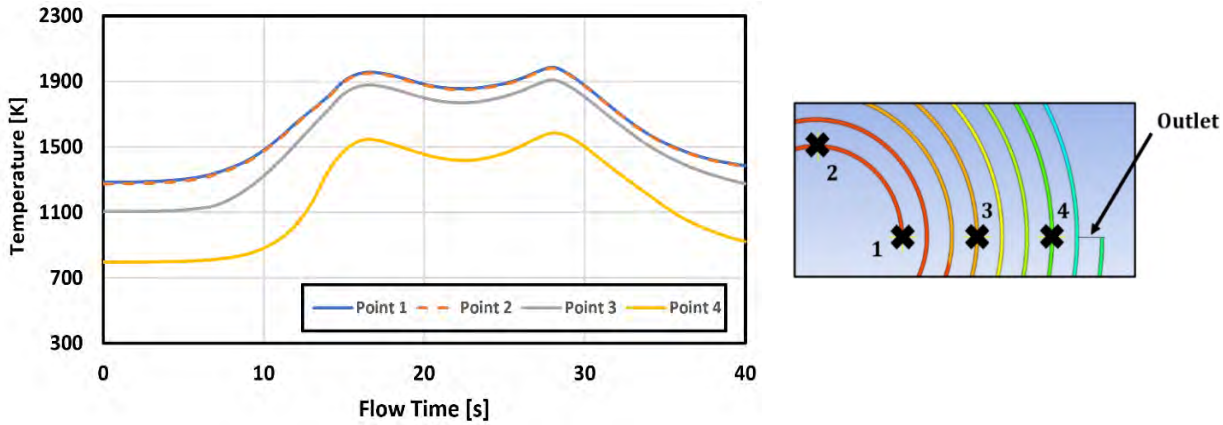

Figure 17: Transient temperature profiles at different locations for $\emptyset_{peak}$ = 2.0 and T_{Surge} = 32s

The revised design space subjected to different transient failure modes is shown qualitatively in **Figure 18**, and quantitatively in **Figure 19**. Insufficient DRE performance limit constraints can be visualized as a relatively narrower envelope compared to conventional extinction limits. For lean to slightly rich mixtures, corresponding to up to a tenfold increase in flare gas, the methane DRE performance holds very close to 99% and is expected to maintain the value for longer surge periods as suggested by the preceding oscillatory-response study. The DRE values progressively fall off significantly for very rich mixtures and eventually result in extinction. For brief surge durations of less than 16 seconds, the flames can survive through the extinction limits predicted under steady-flow conditions and are able to recover to original conditions despite being subjected to more than a factor of 36 increase in flare gas. As for over-temperature concerns, the total timescales in which the solid domain is exposed to a temperature above material limits were found to be comparable to the overall surge duration.

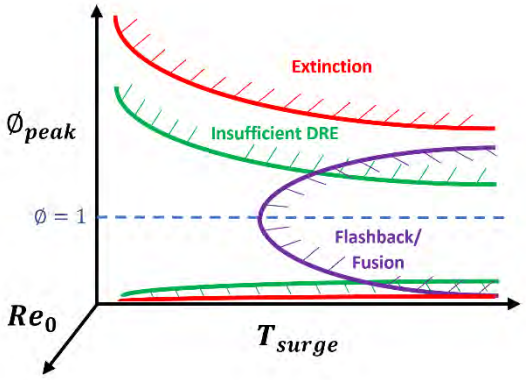

Figure 18: Qualitative design space for Swiss roll combustors visualized across extinction, DRE, and flashback failure mode constraints.

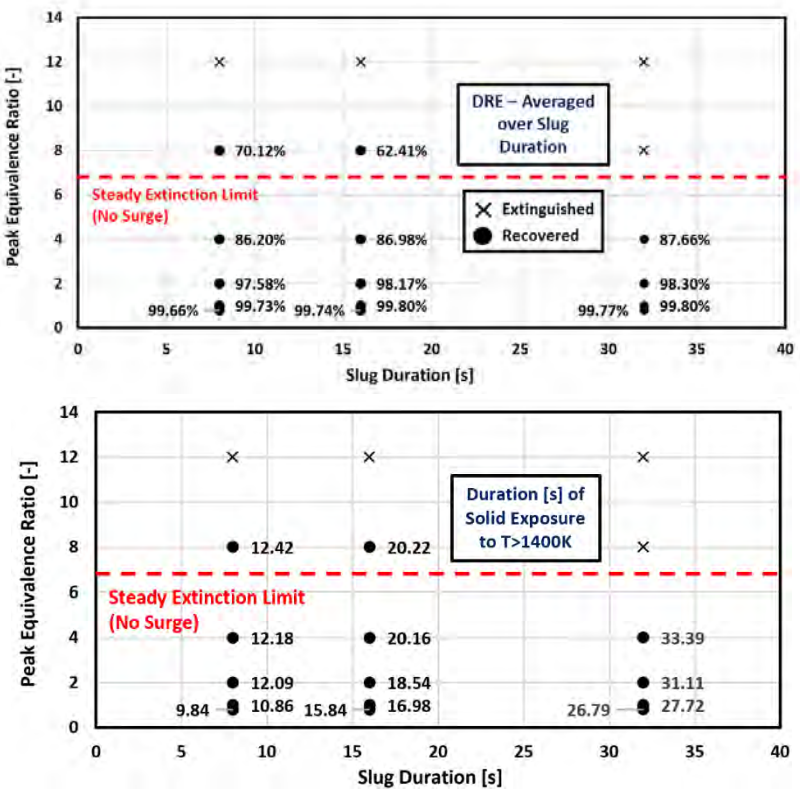

Figure 19: (Top) DRE performance (time-averaged across slug duration) and **(Bottom)** total duration which solid domain is exposed to high temperature under different methane surge profiles ($\emptyset_{peak}$, T_{Surge}) for 3.5 turns combustor operating initially at lean-limit conditions ($\emptyset_0$ = 0.22)

6. Conclusion

An overview of the Swiss roll combustor was presented along with technical features and benefits for flaring applications. CFD models show that the Swiss roll can be designed for flaring under different on-field conditions and constraints (pressure drop, flow rates, and fuel compositions). The performance of the Swiss roll combustor can be tuned by parameters including the channel width, number of turns, and exhaust stack height. The CFD models without reaction chemistry show that the mass flow scales with the hydraulic diameter squared. Additionally, the effects of buoyancy were shown to be sufficient for providing the required airflow for combustion via a natural draft; thus, a fully passive Swiss roll may be viable for certain applications. The oscillatory response from the transient CFD models with detailed chemistry showed the Swiss roll's ability to handle large fluctuations in the flare gas flow rate and composition, potentially simplifying the control system required for the system to ensure high destruction efficiency.

Future work will involve experimental testing of the Swiss roll to confirm the validity of the CFD models, and the findings from these tests will be shared in subsequent publications.

7. Acknowledgements

This research was funded by the Advanced Research Projects Agency-Energy (ARPA-E) under contract number DE-AR0001538. The authors thank the program manager Dr. Jack Lewnard for his support during the project.

8. References

1. Sitton, R.; (2020). *Sitton Texas Flaring Report Q1 2020*. https://www.rrc.texas.gov/media/vhhj43cq/sitton-texas-flaring-report-q1-2020.pdf
2. Lloyd, S.; Weinberg, F. A burner for mixtures of very low heat content. Nature, 1974, 251, 47-49.
3. Jones, A.; Lloyd, S.; Weinberg, F. Combustion in heat exchangers. *Proceedings of the Royal Society of London Section A*, **1978**, 360, 97-115.
4. Ronney, P. Analysis of non-adiabatic heat-recirculating combustors. *Combustion and Flame*, **2003**, 135, 421-439.
5. Chen, C.; Ronney, P. Three-dimensional effects in counterflow heat-recirculating combustors. *Proceedings of the Combustion Institute,* **2011**, 33, 3285-3291.
6. Chen, C.; Ronney, P. Scale and geometry effects on heat-recirculating combustors. *Combustion Theory and Modelling*, **2013**, 17, 888-905.
7. Chen, C.; Ronney, P. Geometrical effects on Swiss roll heat-recirculating combustors. PhD Thesis, University of Southern California, **2011**.
8. Crawmer, J.; Chen, C.; Richard, B.; Pearlman, H.; Edwards, T.; Ronney, P. An Innovative Volatile Organic Compound Incinerator. *International Conference on Thermal Treatment Technologies & Hazardous Waste Combustors*, **2018,** IT3-22
9. G.P. Smith, D.M. Golden, M. Frenklach, N.W. Moriarty, B. Eiteneer, M. Goldenberg, C.T. Bowman, R.K. Hanson, S. Song, W.C.J. Gardiner, V. V. Lissianski, Z. Qin, GRI-Mech 3.0, (2023). http://www.me.berkeley.edu/gri_mech/.